Human Cancer Biology

Clinical Cancer Research

Combined Functional Genome Survey of Therapeutic Targets for Hepatocellular Carcinoma

Reiko Satow[1], Miki Shitashige[1], Yae Kanai[2], Fumitaka Takeshita[3], Hidenori Ojima[2], Takafumi Jigami[1], Kazufumi Honda[1], Tomoo Kosuge[4], Takahiro Ochiya[3], Setsuo Hirohashi[1,2], and Tesshi Yamada[1]

Abstract

Purpose: The outcome of patients with advanced hepatocellular carcinoma (HCC) has remained unsatisfactory. Patients with HCC suffer from chronic hepatitis or liver cirrhosis, and their reserve liver function is often limited.

Experimental Design: To develop new therapeutic agents that act specifically on HCC but interfere only minimally with residual liver function, we searched for genes that were upregulated in 20 cases of HCC [namely, discovery sets 1 (n = 10) and 2 (n = 10)] in comparison with corresponding nontumorous liver and a panel representing normal organs using high-density microarrays capable of detecting all exons in the human genome.

Results: Eleven transcripts whose expression was significantly increased in HCC were subjected to siRNA-based secondary screening of genes required for HCC cell proliferation as well as quantitative reverse transcription-PCR analysis [validation sets 1 (n = 20) and 2 (n = 44)] and immunohistochemistry (n = 19). We finally extracted four genes, *AKR1B10*, *HCAP-G*, *RRM2*, and *TPX2*, as candidate therapeutic targets for HCC. siRNA-mediated knockdown of these candidate genes inhibited the proliferation of HCC cells and the growth of HCC xenografts transplanted into immunodeficient mice.

Conclusions: The four genes we identified were highly expressed in HCC, and HCC cells are highly dependent on these genes for proliferation. Although many important genes must have been overlooked, the selected genes were biologically relevant. The combination of genome-wide expression and functional screening described here is a rapid and comprehensive approach that could be applied in the identification of therapeutic targets in any type of human malignancy. *Clin Cancer Res; 16(9); 2518–28. ©2010 AACR.*

Liver cancer is the fifth most common human cancer worldwide and the third most common cause of cancer mortality. Hepatocellular carcinoma (HCC) is the most common histologic subtype of liver cancer and is highly endemic in Southeast Asia and sub-Saharan Africa (1). HCC develops mainly in liver affected by chronic hepatitis or cirrhosis caused by persistent infection with hepatitis B or C virus; however, the precise molecular mechanisms that drive the transition from the background liver conditions to cancer are largely unknown. Liver resection, ethanol injection, radiofrequency ablation, and chemoembolization have been used successfully for the local management of HCC; however, no single cytotoxic chemotherapeutic agent has been proven effective for the systemic treatment of HCC; thus, the outcome for patients with locally advanced, multicentric, and/or metastatic HCC who are not eligible for these local treatments has remained unsatisfactory.

An increasing number of therapeutic agents targeting molecular components essential for cancer cell growth have begun to be incorporated into oncological practice: Imatinib, which blocks the Bcr-Abl fusion kinase of chronic myeloid leukemia (CML), is currently the first-line therapy for CML (2). The epidermal growth factor receptor inhibitors gefitinib and erlotinib have been used in the treatment of advanced non–small cell lung cancer (3). Recently, it was shown in a phase III study that sorafenib (BAY 43-9006), a multikinase inhibitor, significantly improved the overall survival of patients with advanced HCC (4, 5), and, consequently, sorafenib has since been approved for the treatment of patients with unresectable HCC by the American Food and Drug Administration. However, most patients enrolled in those studies retained relatively well-compensated

Authors' Affiliations: [1]Chemotherapy Division, [2]Pathology Division, and [3]Section for Studies on Metastasis, National Cancer Center Research Institute; and [4]Hepatobiliary and Pancreatic Surgery Division, National Cancer Center Hospital, Tokyo, Japan

Note: Supplementary data for this article are available at Clinical Cancer Research Online (http://clincancerres.aacrjournals.org/).

Microarray data from this study have been submitted to the Gene Expression Omnibus database (accession no. GSE12941).

Corresponding Author: Tesshi Yamada, Chemotherapy Division, National Cancer Center Research Institute, 5-1-1 Tsukiji, Chuo-ku, Tokyo 104-0045, Japan. Phone: 81-3-3542-2511; Fax: 81-3-3547-6045; E-mail: tyamada@ncc.go.jp.

doi: 10.1158/1078-0432.CCR-09-2214

©2010 American Association for Cancer Research.

Translational Relevance

Liver cancer is the fifth most common human cancer worldwide and the third most common cause of cancer mortality. Recently, a multikinase inhibitor, sorafenib, has been approved as a systemic chemotherapeutic drug for advanced hepatocellular carcinoma (HCC); however, further improvement seems to be necessary. To identify an "Achilles heel" of HCC cells and develop new therapeutic agents that act specifically on HCC but interfere only minimally with residual liver function, we performed an unbiased survey of the whole genome. We finally identified four genes as candidates. siRNA-mediated knockdown of these candidate genes inhibited the proliferation of HCC cells and the growth of HCC xenografts transplanted into immunodeficient mice, confirming their feasibility as therapy targets.

liver function. In reality, the reserve liver function of HCC patients is often limited due to underlying liver conditions. Therefore, the safety and tolerability of sorafenib remain to be determined in HCC patients with compromised liver function. Therapeutic targeting molecules other than protein kinases have also been developed against various tumors of other organs (6–8). To identify a molecule essential for HCC cell growth and develop new therapeutic agents that would act specifically on HCC and only minimally interfere with residual liver function, a survey of the whole genome would be necessary.

In this study, we adopted a combined functional approach. We first searched for genes that were upregulated in HCC in comparison with the background nontumorous liver tissue. This was followed by siRNA-based screening of genes required for HCC cell proliferation. Recently, whole-genome RNA interference (RNAi)–based functional screening has been reported to successfully identify genes that sensitize lung cancer cells to a chemotherapeutic drug and genes required for proliferation and survival of several cancer cell lines; however, in those studies, the expressional specificity of the identified targets was not taken into consideration (9–12). Here, we report the identification of possible therapeutic target molecules of HCC through a combination of genome-wide expression and functional screening.

Materials and Methods

Patients and microarray analysis. Samples of HCC and surrounding nontumorous liver tissue were collected from 84 patients who underwent liver resection for HCC at the National Cancer Center Hospital (Tokyo, Japan) with informed consent. The clinical and histologic data for these patients are summarized in Supplementary Table S1. Total RNA of normal human organs was obtained from a commercial source (FirstChoice Human Total RNA Survey Panel, Ambion).

One microgram of total RNA was converted to end-labeled cRNA using a Whole Transcript Sense Target Labeling kit (Affymetrix). The fluorescent cRNA probes were hybridized to Human Exon 1.0 ST arrays (Affymetrix), as instructed by the supplier. Data analysis was carried out using the ArrayAssist software package (version 5.5.1, Stratagene). A GC content-based background correction followed by quantile normalization was done with an exonRMA algorithm available in the package. Multiple exonic expression data were also summarized into a single value using the same algorithm, as instructed by the supplier (http://www.stratagene.com/manuals/ArrayAssist.pdf).

The protocol of this study was reviewed and approved by the ethics committee of the National Cancer Center (Tokyo, Japan).

Cell lines. Three human cell lines derived from HCC were used in this study. KIM-1 was kindly provided by Dr. Masamichi Kojiro (Kurume University, Kurume, Japan). Hep3B was obtained from the Cell Resource Center for Biomedical Research, Tohoku University (Sendai, Japan). HLE was obtained from the Health Science Research Resources Bank (Osaka, Japan). KIM-1 and Hep3B were maintained in RPMI 1640 (Invitrogen) supplemented with 10% fetal bovine serum. HLE was maintained in Dulbecco's modified Eagle's medium (Invitrogen) supplemented with 10% fetal bovine serum.

siRNA-based functional screening. The day before siRNA transfection, cells were seeded at 5×10^3 per well in 96-well plates to obtain 50% to 60% confluency. They were then transfected with siRNA using Lipofectamine 2000 (Invitrogen) at a concentration of 10, 20, or 50 nmol/L in KIM1, Hep3B, or HLE cells, respectively. Three days later, the relative proportion of living cells was assessed using a Premix WST-1 Cell Proliferation Assay System (Takara Bio) in accordance with the manufacturer's instructions. The siRNA was synthesized by Ambion, and the identification (ID) numbers of siRNAs used in this study are listed in Supplementary Table S4. Silencer Negative Control #1 siRNA (Ambion) was used as a nontargeting control. siRNA targeting *TOP2A* was described previously (13).

Real-time PCR. First-strand cDNA was synthesized from 1 μg of total RNA using SuperScript reverse transcriptase (Invitrogen). Real-time PCR was done as described previously (14). Primers and probes sets were obtained from Applied Biosystems, and their Assay IDs are provided in Supplementary Table S5. The amplification reaction was done according to the manufacturer's instructions (95°C for 10 minutes followed by 40 cycles of 95°C for 15 seconds, 50°C for 2 minutes, and 60°C for 1 minute).

Immunohistochemistry and immunoblot analysis. Anti-AKR1B10 (clone 1A6) and anti–HCAP-G (clone 4B1) monoclonal antibodies were purchased from Abnova. Anti-RRM2 antibody (E-16) was purchased from Santa

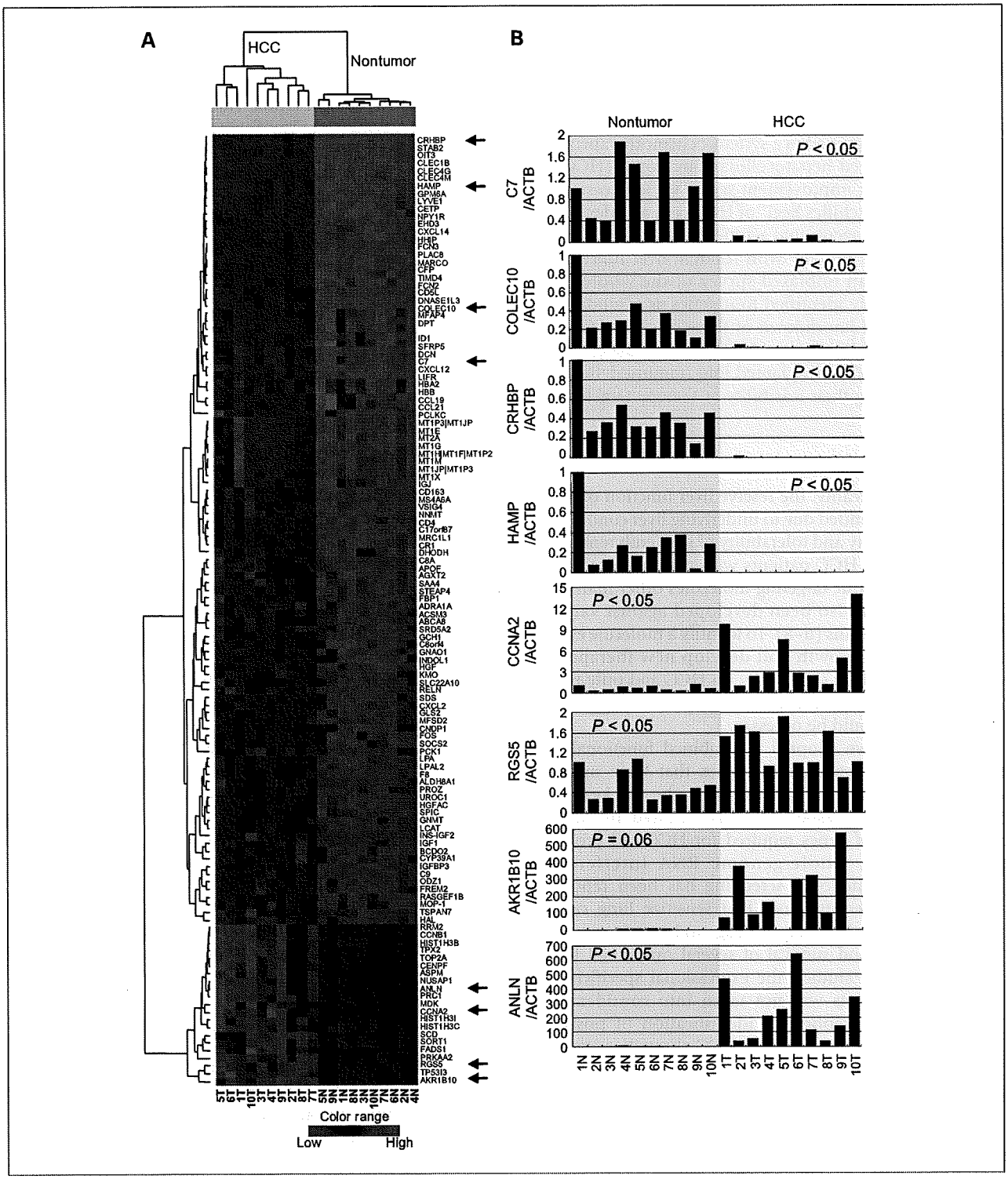

Fig. 1. Genes differentially expressed between HCC and nontumorous liver. A, hierarchical clustering of 124 genes whose expression differed significantly ($P < 0.001$ and >3-fold change) between HCC and adjacent nontumorous liver. Transcriptional signal intensity is shown as a heat map. Red indicates higher signals, whereas blue indicates lower signals. Arrows indicate eight genes selected for validation by real-time PCR (B). B, validation of the microarray data by real-time RT-PCR. The expression levels of eight representative genes whose expression differed significantly between adjacent nontumorous liver (left) and HCC (right) were validated by real-time RT-PCR (shown in arbitrary units). Significant correlation between array (discovery set 1) and real-time RT-PCR data was confirmed by calculating correlation coefficient values in eight randomly selected genes (indicated by arrows in A): *C7*, 0.96; *COLEC10*, 0.97; *CRHBP*, 0.98; *HAMP*, 0.98; *CCNA2*, 0.82; *RGS5*, 0.80; *AKR1B10*, 0.98; *ANLA*, 0.92. The significance of differential expression between HCC and adjacent nontumorous liver tissue was assessed using a permutation paired *t* test, and Bonferroni-corrected *P* values are provided.

Cruz Biotechnology. Anti-TPX2 antibody was purchased from Novus Biologicals.

Formalin-fixed and paraffin-embedded liver tissues containing HCC were obtained from the National Cancer Center Hospital, and stained as described previously (15, 16). Immunoblot analysis of the KIM-1 cell lysate was done as described previously (15).

Animal experiments. Eight million KIM-1 cells suspended in 0.1 mL of PBS were s.c. inoculated into the flanks of 5-week-old female BALB/c nu/nu nude mice (SLC). Eight days later, the tumor-bearing mice were treated with siRNA together with atelocollagen (Koken Co., Ltd.), as described previously (17, 18). The final concentration of siRNA and atelocollagen was 11 μmol/L and 0.5%, respectively, and 200 μL of the siRNA solution were injected directly into each tumor. Tumor volume was determined every 3 days using the formula $V = 1/2\ (A \times B^2)$, where A and B represent the largest and smallest dimensions of the tumor, respectively.

Animal experiments were reviewed by the institutional ethics committee and performed in compliance with the

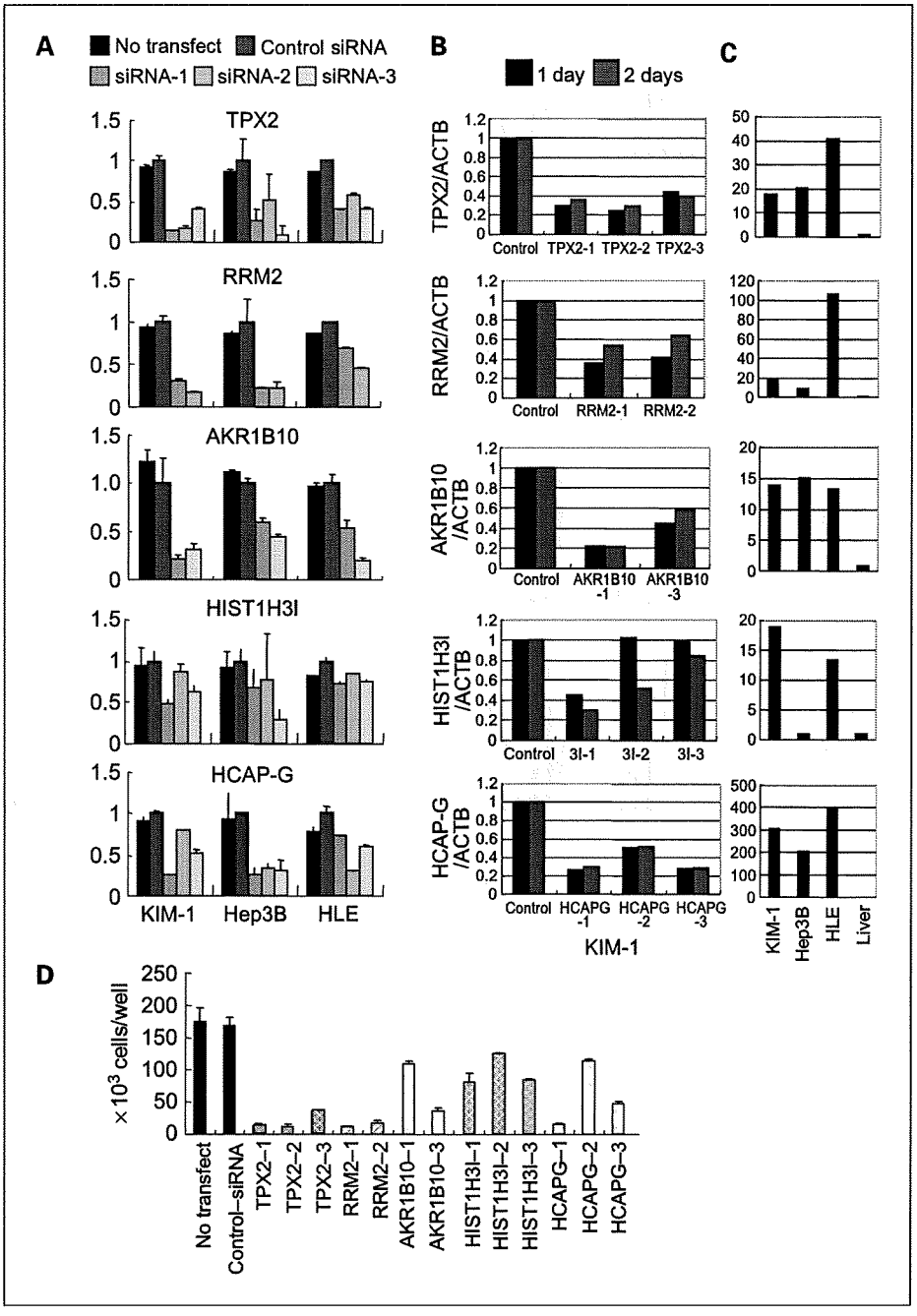

Fig. 2. siRNA-based functional screening. A, siRNA-mediated screening of genes required for proliferation of HCC cells. Three HCC cell lines (KIM-1, Hep3B, and HLE) were transfected with the indicated siRNAs, and the relative proportion of living cells was assessed 3 days later by measuring the mitochondrial succinate-tetrazolium reductase activity. Values for control siRNA were set at 1. B, reduction of the level of mRNA for each gene was determined by real-time PCR 1 and 2 days after transfection of KIM-1 cells with the indicated siRNAs. Values for control siRNA were set at 1. C, expression of each gene in HCC cell lines (KIM-1, Hep3B, and HLE) and normal liver tissue. D, confirmation of siRNA-mediated inhibition of HCC cell proliferation. KIM-1 cells were transfected with the indicated siRNAs, and the number of living cells was counted 3 days later by trypan blue dye exclusion using a hemocytometer.

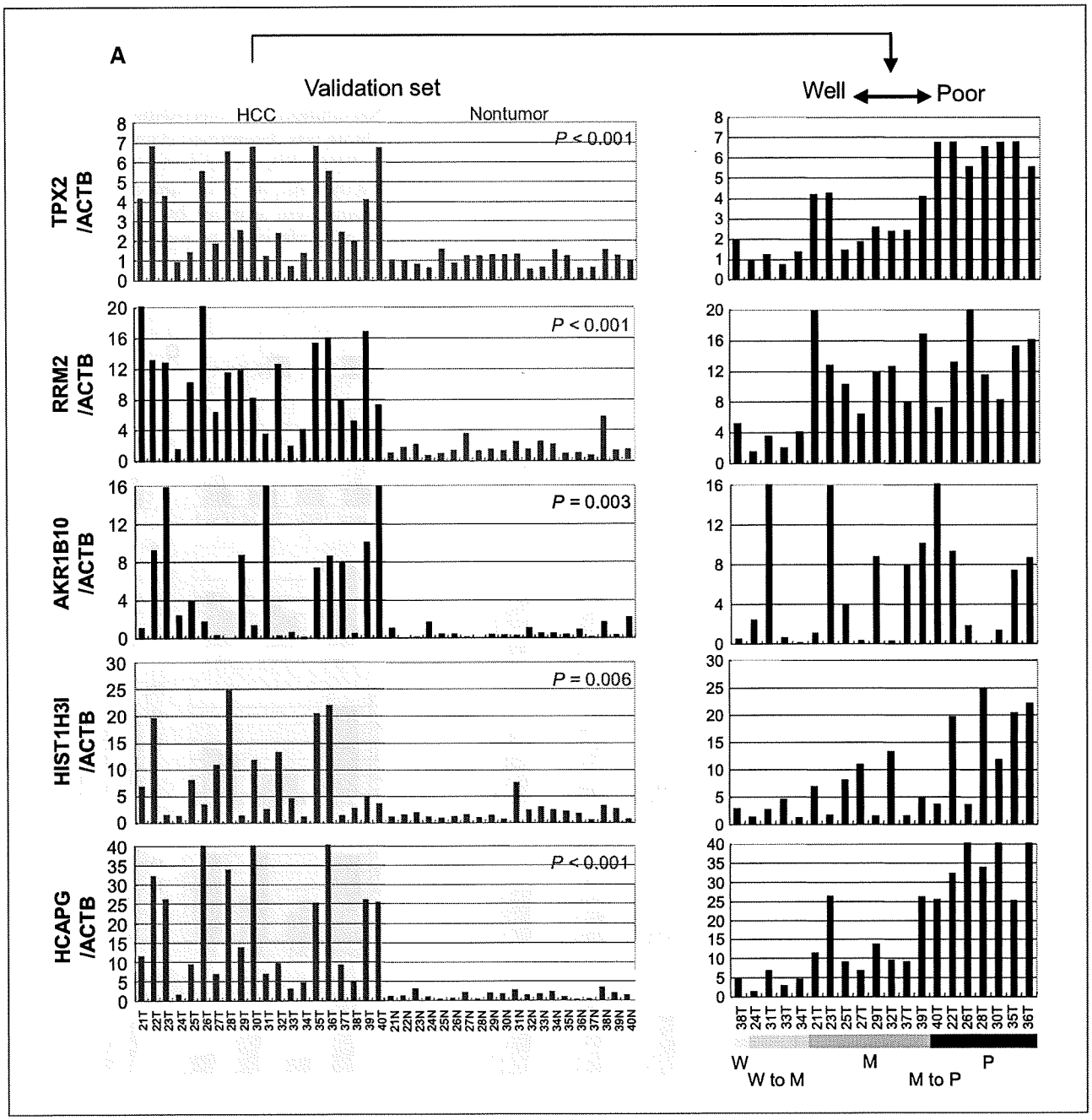

Fig. 3. Validation of differential expression. A, mRNA expression levels of selected genes in 20 independent pairs of HCC (21-40T) and adjacent nontumorous liver tissue (21-40N; validation set 1) determined by real-time PCR (left). The expression levels in HCC were realigned according to histologic differentiation (right). W, well differentiated; W to M, well to moderately differentiated; M, moderately differentiated; M to P, moderately to poorly differentiated, P, poorly differentiated.

guidelines for Laboratory Animal Research of the National Cancer Center Research Institute (Tokyo, Japan).

Statistical analysis. To extract differentially expressed genes from the array data, a paired *t* test with no correction was done (19) with asymptotic distribution to determine the *P* value. Correlations between array data and real-time PCR measurements were assessed using the Pearson correlation coefficient. The significance of differential gene expression between HCC and adjacent nontumorous liver tissue was assessed using the permutation paired *t* test followed by Bonferroni correction.

The weights and volumes of tumors are given as means (+SE). To evaluate the chronological effect of siRNAs on the growth of xenografts in comparison with control siRNA,

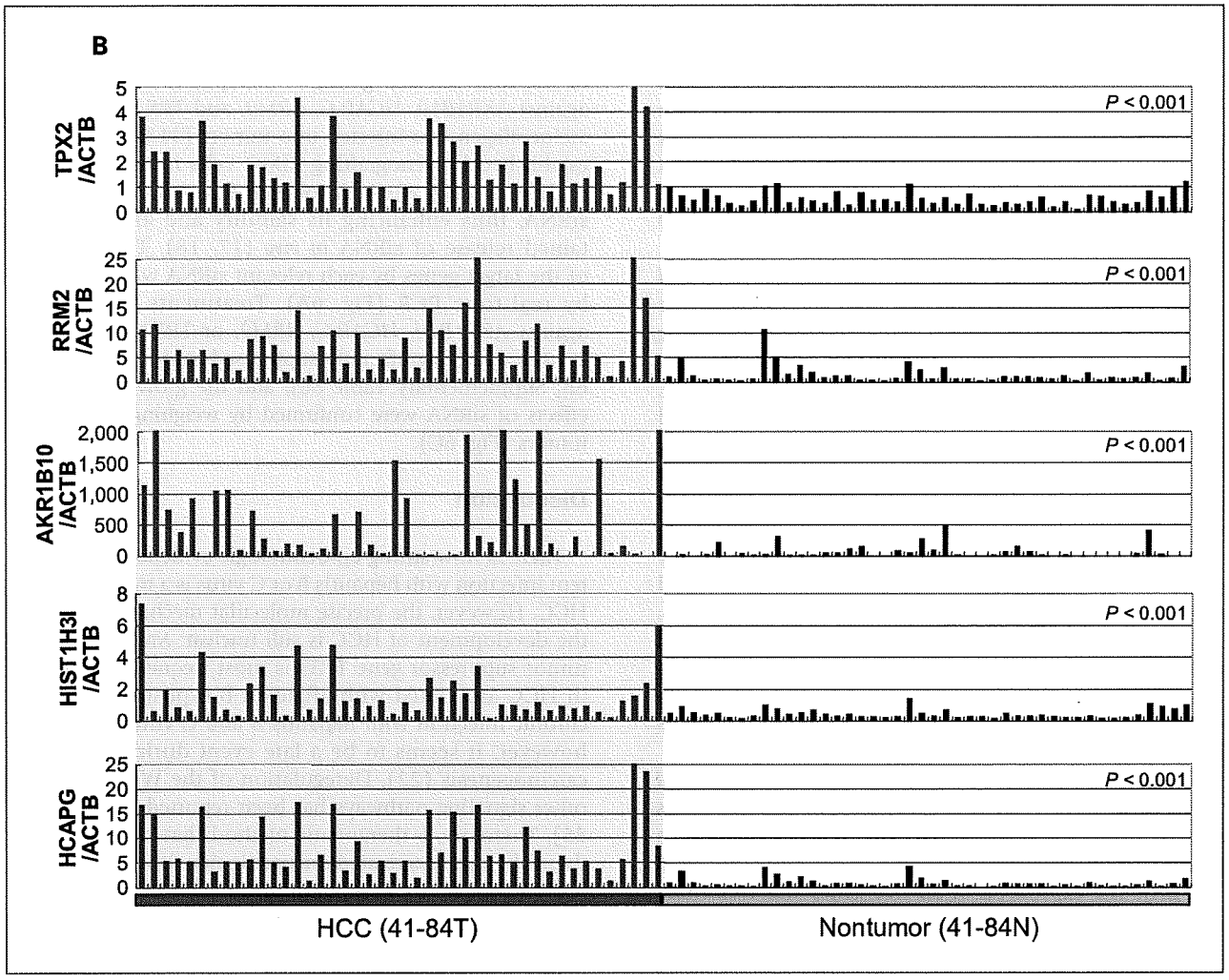

Fig. 3. ***Continued.*** B, expression levels of mRNAs for selected genes in 44 independent pairs of HCC (41-84T) and adjacent nontumorous liver tissue (41-84N; validation set 2) determined by real-time PCR.

a generalized linear mixed-effects model was used (20). The volume of the xenograft was modeled using γ-error distribution and log link function. This model considers each siRNA treatment as a fixed effect with control siRNA as an intercept and the number of days after implantation as a random effect. Estimates of variance components were obtained using the Laplacian approximation method, and the model fit was assessed using deviances. The significance of effects was estimated from the degree of freedom and t statistics followed by Bonferroni correction. Analysis was done using the lmer function for fitting generalized linear mixed-effects models, in the R statistical software package (version 2.6.0).

Results

Exon-based array analysis of HCC. Twenty paired samples of HCC and adjacent nontumorous liver tissue were subjected to genome-wide expression analysis using two different batches of the GeneChip Human Exon 1.0 ST arrays [discovery sets 1 (10 pairs) and 2 (10 pairs)]. Statistical analysis was done separately, and genes expressed differentially in the two sets were selected to eliminate any experimental bias caused by batch-to-batch variations. The exon array can detect mRNAs with low abundance as well as alternatively polyadenylated and spliced mRNA because the probes are designed to hybridize with the entire sequences of the transcripts (21). We identified 124 annotated genes that were differentially expressed between the background (nontumorous) liver tissue and HCC [at least a 3-fold change in transcription signal; $P < 0.001$ (paired t test with no correction)] in discovery set 1 (Supplementary Tables S2 and S3). The genes were clustered according to the similarity of their expression profiles (Fig. 1A), and the differential expression of representative genes was confirmed by real-time PCR (Fig. 1B). It was noteworthy that although 103 genes were found to be significantly downregulated, only 21 were apparently upregulated.

We selected 9 genes (*AKR1B10*, *ANLN*, *CCNB1*, *HIST1H3B*, *HIST1H3C*, *HIST1H3I*, *RRM2*, *TOP2A*, and *TPX2*) whose expression was upregulated in HCC (≥3-fold change in transcription signal; $P < 0.001$, t test) in both discovery sets 1 and 2. Furthermore, two additional genes (*HCAP-G* and *DEPDC1*) were selected using a different criterion (>2.5-fold change across all of the 20 cases in discovery sets 1 and 2, and a raw signal of <50 in all 20 of the nontumorous liver tissues; $P < 0.05$, t test).

RNAi-based screening of genes required for HCC cell proliferation. To identify genes that are essential for HCC cell proliferation, siRNA-based screening was done for the 11 genes that were upregulated in HCC. Two or three constructs of siRNA were designed for each gene. Relative cell viability was evaluated by the mitochondrial succinate-tetrazolium reductase activity-based assay 3 days after transfection (Fig. 2A). We selected five genes (*TPX2*, *RRM2*, *HCAP-G*, *HIST1H3I*, and *AKR1B10*) based on the criterion that at least two siRNAs per gene reproducibly suppressed cell proliferation by >20% in all of three cell lines (KIM-1, Hep3B, and HLE). Representative data are shown in Fig. 2A and B. The baseline expression of these genes was determined in the three cell lines by real-time reverse transcription-PCR (RT-PCR; Fig. 2C). We confirmed the cell proliferation–inhibitory activity of the siRNA by counting the numbers of cells (Fig. 2D).

Validation of differential gene expression in additional cases of HCC. The increased expression of the five genes selected using the siRNA-based screen was validated in 20 cases of HCC (validation set 1) by real-time PCR (Fig. 3A). The expression of all five genes was confirmed to be increased in HCC. The expression of *TPX2*, *RRM2*, *HCAP-G*, and *HIST1H3* was associated with loss of histologic differentiation (Fig. 3A, right). The expression of *AKR1B10* was upregulated in HCC regardless of differentiation. We further confirmed the differential expression of these genes between HCC and nontumorous liver tissues in 44 additional independent cases of HCC (validation set 2) by real-time PCR (Fig. 3B).

In the 18 normal organs examined, no significant expression of *TPX2*, *RRM2*, or *HCAP-G* was observed, except for the thymus (Fig. 4, left), which is largely involuted in nonjuvenile adults. No organs showed higher expression of *AKR1B10* than was the case in HCC. We did not select *HIST1H3I*, as this gene showed high expression in several vital organs (Fig. 4).

Protein expression analysis. Expression of the products of four candidate genes, *TPX2*, *HCAP-G*, *RRM2*, and *AKR1B10*, was examined immunohistochemically in 19 independent cases of HCC (Fig. 5). In 84% (16 of 19) of the cases, AKR1B10 protein was detected in the cancer but was hardly evident in the adjacent nontumorous liver tissue. The nuclear staining of HCAP-G and TPX2 was stronger in HCC than in the adjacent nontumorous liver in 42% (8 of 19) and 58% (11 of 19) of cases, respectively. Patchy staining of RRM2 was observed in 84% (16 of 19) of the HCCs.

***Inhibition of tumor growth* in vivo.** Finally, we performed an *in vivo* experiment to evaluate the feasibility of the four selected genes as therapeutic targets. siRNA against *AKR1B10*, *HCAP-G*, *RRM2*, and *TPX2* mixed with atelocollagen was injected into tumors (31.5 ± 1.9 mm^3) established by xenografting KIM-1 cells into the flank of nude mice (Fig. 6). Atelocollagen forms a complex with siRNA, thus enhancing its stability and allowing sustained release of siRNA *in vivo* (17, 18). The silencing of the target genes by each relevant siRNA was confirmed by real-time PCR (Fig. 6A). Treatments with siRNA against *AKR1B10*, *HCAP-G*, *RRM2*, or *TPX2* given twice, 1 week apart, significantly suppressed tumor growth (Fig. 6B; Supplementary Table S6), and the growth-inhibitory effects of siRNA were confirmed by weighing the excised tumors (Fig. 6C).

Discussion

There is now strong epidemiologic evidence that persistent infection with hepatitis B or C virus is a major cause of HCC. However, the precise molecular mechanism behind the development of HCC is still unclear. Mutation in the tumor suppressor gene *TP53* is most frequently observed in HCC associated with aflatoxin B exposure as well as chronic infection with hepatitis B and C viruses (22–24); however, it seems to be a late event during multistep carcinogenesis (22). Deregulation of the Wnt as well as other signaling pathways has been reported in HCC (22, 25). Therefore, a therapeutic method that can normalize these aberrantly activated oncogenic signals would be clinically valuable. In an attempt to discover therapeutic targets with high specificity for HCC, we searched for genes that are specifically upregulated in HCC in comparison with nontumorous liver tissue and normal vital organs using high-density microarrays designed to detect all the exons in the human genome (Figs. 1 and 4). This was followed by siRNA-based screening of genes required for HCC cell proliferation (Fig. 2) as well as quantitative RT-PCR analysis and immunohistochemistry of additional cases (Figs. 3 and 5). We finally identified four candidate genes and confirmed their functional involvement in the tumor growth of HCC xenografts (Fig. 6). These genes, *AKR1B10*, *HCAP-G*, *RRM2*, and *TPX2*, were expressed strongly and specifically in HCC, which is highly dependent on these genes for proliferation, and their feasibility as therapy targets also seems to be supported by the literature.

RRM2 is a subunit of ribonucleotide reductase that catalyzes the conversion of ribonucleoside 5′-diphosphates into their corresponding 2′-deoxyribonucleotides. Because this reaction is the rate-limiting step of DNA synthesis, and inhibition of ribonucleotide reductase stops DNA synthesis and cell proliferation, RRM2 has been considered a promising target for cancer therapy (26).

TPX2 (C20ORF1) is a microtubule-associated protein whose expression is restricted to the S, G_2, and M phases of the cell cycle. Suppression of TPX2 expression by RNAi causes defects in microtubule organization during mitosis,

leading to the formation of two microtubule asters that do not form a spindle (27). TPX2 is necessary for maintaining aurora A kinase in an active conformation (28, 29). Aurora kinases are essential for the regulation of chromosome segregation and cytokinesis during mitosis and have been reported to be overexpressed in a wide range of human tumors. Several aurora kinase inhibitors, such as VX-680/MK-0457, have been showed to have anticancer effects *in vitro* and *in vivo* (30, 31). The binding of TPX2 modulates the conformation of aurora A and reduces its affinity

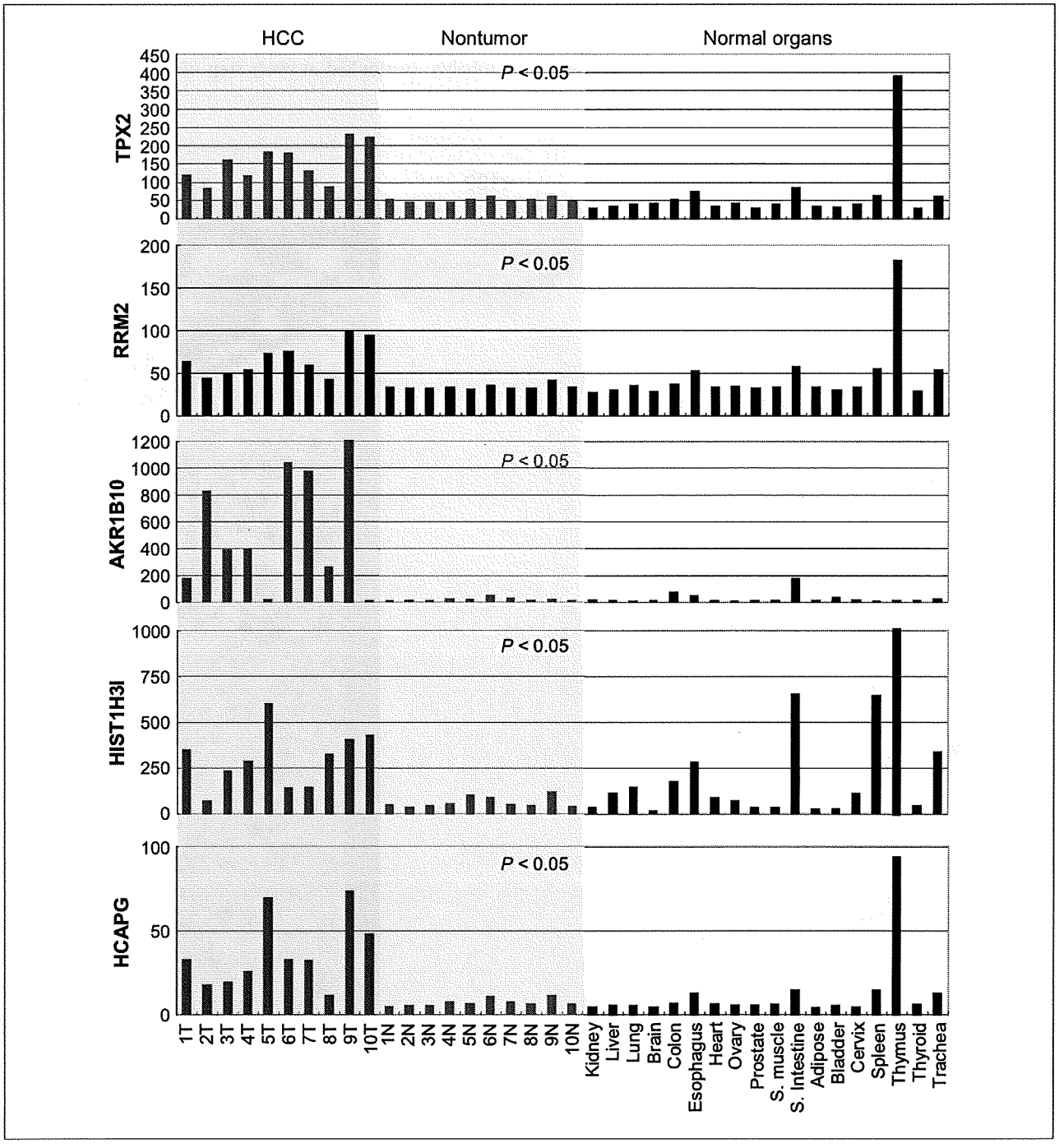

Fig. 4. Expression in normal organs. Expression levels of mRNAs for selected genes in 10 pairs of HCC (1-10T) and adjacent nontumorous liver tissue (1-10N; discovery set 1) and 18 normal organs determined by Human Exon 1.0 ST arrays (shown in arbitrary units). The significance of differential expression between HCC and adjacent nontumorous liver tissue was assessed using permutation paired *t* test, and Bonferroni-corrected *P* values are provided. S. muscle, skeletal muscle; S. intestine, small intestine.

for VX-680 (32). Inhibition of TPX2 may increase the efficacy of this class of aurora kinase inhibitors.

HCAP-G is a component of the condensin complex that organizes the coiling topology of individual chromatids. Condensin also contributes to mitosis-specific chromosome compaction and is required for proper chromosome segregation, although the functional significance of HCAP-G in the condensing complex is largely unknown (33, 34).

AKR1B10 (ARL1, aldose reductase-like 1) was originally isolated as a new member of the aldo-keto reductase superfamily overexpressed in HCC and is reportedly related to the histologic differentiation of HCC (35, 36). AKR1B10 was also overexpressed in squamous cell carcinoma of the lung and its precursor conditions (37). Because the expression of AKR1B10 was highly specific to HCC and its inhibition suppressed tumor growth (Fig. 6), chemicals that specifically inhibit AKR1B10 activity may be useful anticancer drugs with minimal side effects.

It cannot be denied that many important genes were probably overlooked at every step of the present screen,

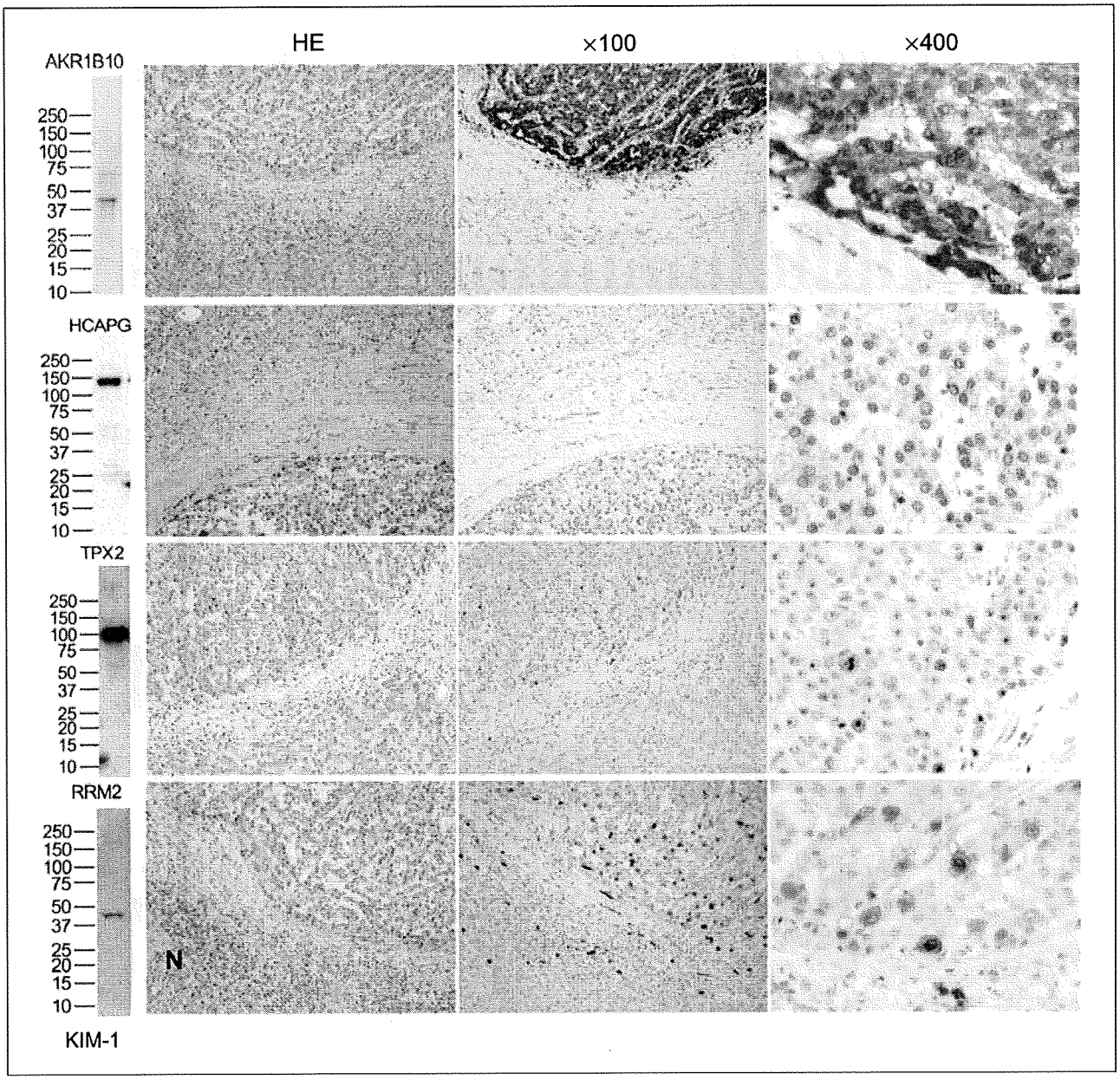

Fig. 5. Protein expression in HCC. Hematoxylin and eosin (HE) staining (original magnification, × 100) and immunoperoxidase staining (original magnifications, × 100 and × 400) of AKR1B10, HCAP-G, RRM2, and TPX2 proteins in HCC and adjacent nontumorous liver tissue. The specificity of antibodies was determined by immunoblotting of the KIM-1 cell lysate (left). N, nontumorous liver.

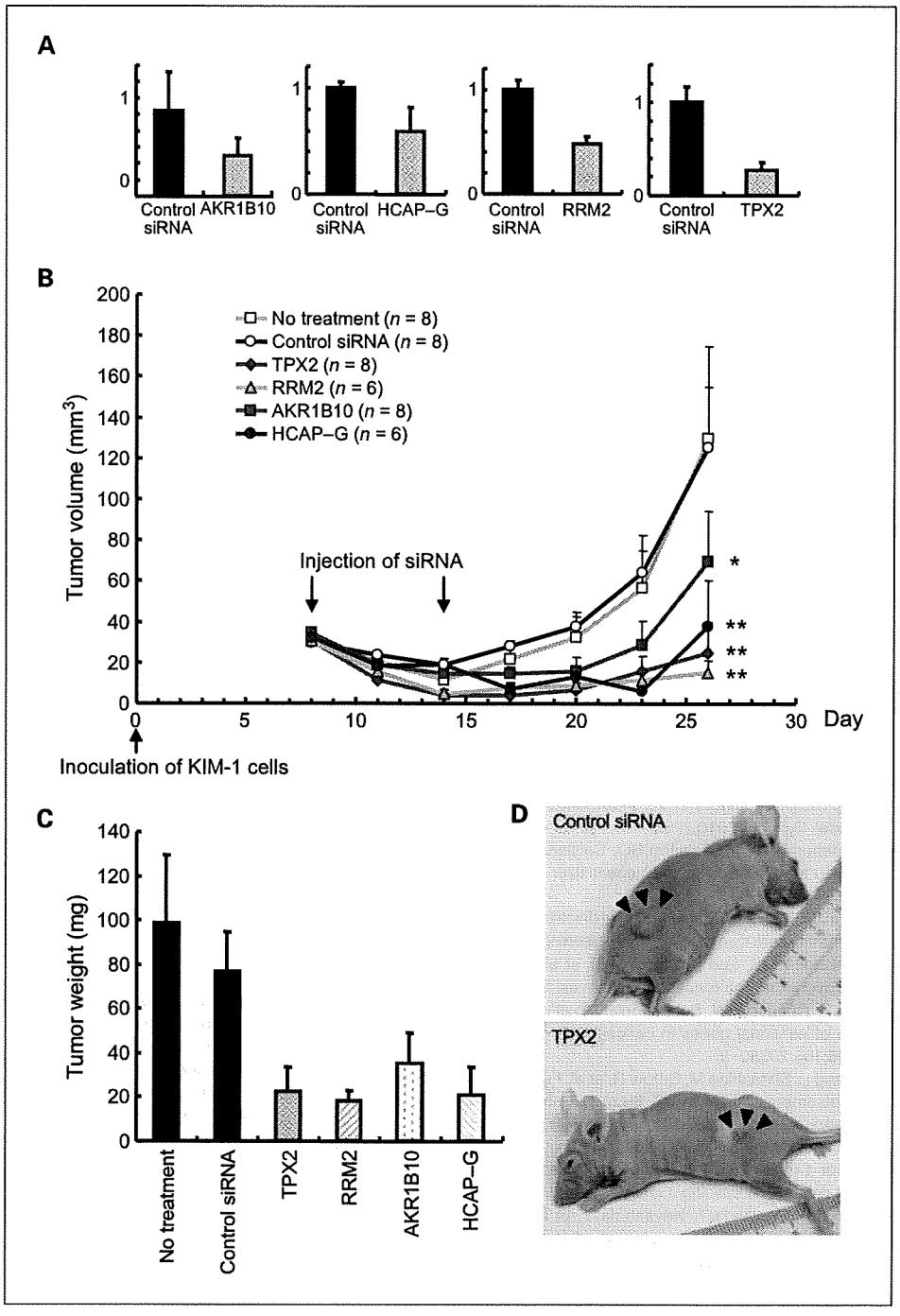

Fig. 6. Suppression of tumor growth by siRNA. A, KIM-1 cells were s.c. inoculated into the flanks of nude mice. Eight days later, control siRNA or siRNA against *AKR1B10, HCAP-G, RRM2*, or *TPX2* was injected into the developed tumors. The tumors were excised 2 days after the injection, and the expression levels of the indicated genes were determined by real-time PCR. Values of control siRNA were set at 1. B, chronological changes in tumor volume after two injections of the indicated siRNA. Volume of tumors was determined every 3 days as described in Materials and Methods. **, significantly different with a Bonferroni-corrected *P* value of <0.001. *, significantly different with a Bonferroni-corrected *P* value of 0.012. C, weight (mean + SE in mg) of xenografts measured 18 days after the second injection of the indicated siRNA and controls. D, macroscopic appearance of xenografts injected with control siRNA (top) and siRNA against TPX2 (bottom).

although the four selected genes seem to be highly relevant from a biological viewpoint. HCC has been recognized as a single category of disease; however, the overall gene expression patterns seem to differ markedly among individual cases. A search for the genes responsible for the different clinical outcomes of HCC will be the subject of a future study. We used the cell proliferation assay for siRNA-based functional screening. However, the use of other assays capable of evaluating cell motility, migration, drug sensitivity, or cell death may help to identify genes differing in their biological significance. The combination of genome-wide expression and functional screening described here provides a rapid and comprehensive approach that could be applicable for studies of various aspects of human cancer.

Disclosure of Potential Conflicts of Interest

No potential conflicts of interest were disclosed.

Acknowledgments

We thank Dr. Masamichi Kojiro (Kurume University, Kurume, Japan) for providing the KIM-1 cells.

Grant Support

Program for Promotion of Fundamental Studies in Health Sciences conducted by the National Institute of Biomedical Innovation of Japan, the Third-Term Comprehensive Control Research for Cancer conducted by the Ministry of Health, Labor and Welfare of Japan, and generous grants from the Natio Foundation and the Princess Takamatsu Cancer Research Fund. These fund resources did not influence the study design or interpretation of the results.

The costs of publication of this article were defrayed in part by the payment of page charges. This article must therefore be hereby marked *advertisement* in accordance with 18 U.S.C. Section 1734 solely to indicate this fact.

Received 08/15/2009; revised 02/01/2010; accepted 03/08/2010; published OnlineFirst 04/13/2010.

References

1. El-Serag HB, Rudolph KL. Hepatocellular carcinoma: epidemiology and molecular carcinogenesis. Gastroenterology 2007;132:2557–76.
2. Hernandez-Boluda JC, Cervantes F. Imatinib mesylate (Gleevec, Glivec):a new therapy for chronic myeloid leukemia and other malignancies. Drugs Today (Barc) 2002;38:601–13.
3. Fong T, Morgensztern D, Govindan R. EGFR inhibitors as first-line therapy in advanced non-small cell lung cancer. J Thorac Oncol 2008;3:303–10.
4. Llovet JM, Ricci S, Mazzaferro V, et al. Sorafenib in advanced hepatocellular carcinoma. N Engl J Med 2008;359:378–90.
5. Di Maio M, Daniele B, Perrone F. Targeted therapies: role of sorafenib in HCC patients with compromised liver function. Nat Rev Clin Oncol 2009;6:505–6.
6. Hideshima T, Chauhan D, Richardson P, Anderson KC. Identification and validation of novel therapeutic targets for multiple myeloma. J Clin Oncol 2005;23:6345–50.
7. Izzo F, Marra P, Beneduce G, et al. Pegylated arginine deiminase treatment of patients with unresectable hepatocellular carcinoma: results from phase I/II studies. J Clin Oncol 2004;22:1815–22.
8. Drew Y, Plummer R. The emerging potential of poly(ADP-ribose) polymerase inhibitors in the treatment of breast cancer. Curr Opin Obstet Gynecol 2010;22:67–71.
9. Whitehurst AW, Bodemann BO, Cardenas J, et al. Synthetic lethal screen identification of chemosensitizer loci in cancer cells. Nature 2007;446:815–9.
10. Silva JM, Marran K, Parker JS, et al. Profiling essential genes in human mammary cells by multiplex RNAi screening. Science 2008;319:617–20.
11. Schlabach MR, Luo J, Solimini NL, et al. Cancer proliferation gene discovery through functional genomics. Science 2008;319:620–4.
12. Luo B, Cheung HW, Subramanian A, et al. Highly parallel identification of essential genes in cancer cells. Proc Natl Acad Sci U S A 2008;105:20380–5.
13. Huang L, Shitashige M, Satow R, et al. Functional interaction of DNA topoisomerase IIα with the β-catenin and T-cell factor-4 complex. Gastroenterology 2007;133:1569–78.
14. Shitashige M, Naishiro Y, Idogawa M, et al. Involvement of splicing factor-1 in β-catenin/T-cell factor-4-mediated gene transactivation and pre-mRNA splicing. Gastroenterology 2007;132:1039–54.
15. Honda K, Yamada T, Hayashida Y, et al. Actinin-4 increases cell motility and promotes lymph node metastasis of colorectal cancer. Gastroenterology 2005;128:51–62.
16. Yamaguchi U, Nakayama R, Honda K, et al. Distinct gene expression-defined classes of gastrointestinal stromal tumor. J Clin Oncol 2008;26:4100–8.
17. Minakuchi Y, Takeshita F, Kosaka N, et al. Atelocollagen-mediated synthetic small interfering RNA delivery for effective gene silencing *in vitro* and *in vivo*. Nucleic Acids Res 2004;32:e109.
18. Takeshita F, Minakuchi Y, Nagahara S, et al. Efficient delivery of small interfering RNA to bone-metastatic tumors by using atelocollagen *in vivo*. Proc Natl Acad Sci U S A 2005;102:12177–82.
19. Shi L, Reid LH, Jones WD, et al. The MicroArray Quality Control (MAQC) project shows inter- and intraplatform reproducibility of gene expression measurements. Nat Biotechnol 2006;24:1151–61.
20. Bolker BM, Brooks ME, Clark CJ, et al. Generalized linear mixed models: a practical guide for ecology and evolution. Trends Ecol Evol 2009;24:127–35.
21. Gardina PJ, Clark TA, Shimada B, et al. Alternative splicing and differential gene expression in colon cancer detected by a whole genome exon array. BMC Genomics 2006;7:325.
22. Hussain SP, Schwank J, Staib F, Wang XW, Harris CC. TP53 mutations and hepatocellular carcinoma: insights into the etiology and pathogenesis of liver cancer. Oncogene 2007;26:2166–76.
23. Gouas D, Shi H, Hainaut P. The aflatoxin-induced TP53 mutation at codon 249 (R249S): biomarker of exposure, early detection and target for therapy. Cancer Lett 2009;286:29–37.
24. Villanueva A, Newell P, Chiang DY, Friedman SL, Llovet JM. Genomics and signaling pathways in hepatocellular carcinoma. Semin Liver Dis 2007;27:55–76.
25. Katoh H, Shibata T, Kokubu A, et al. Genetic inactivation of the APC gene contributes to the malignant progression of sporadic hepatocellular carcinoma: a case report. Genes Chromosomes Cancer 2006;45:1050–7.
26. Shao J, Zhou B, Chu B, Yen Y. Ribonucleotide reductase inhibitors and future drug design. Curr Cancer Drug Targets 2006;6:409–31.
27. Gruss OJ, Vernos I. The mechanism of spindle assembly: functions of Ran and its target TPX2. J Cell Biol 2004;166:949–55.
28. Bayliss R, Sardon T, Ebert J, Lindner D, Vernos I, Conti E. Determinants for Aurora-A activation and Aurora-B discrimination by TPX2. Cell Cycle 2004;3:404–7.
29. Marumoto T, Zhang D, Saya H. Aurora-A—a guardian of poles. Nat Rev Cancer 2005;5:42–50.
30. Keen N, Taylor S. Aurora-kinase inhibitors as anticancer agents. Nat Rev Cancer 2004;4:927–36.
31. Harrington EA, Bebbington D, Moore J, et al. VX-680, a potent and selective small-molecule inhibitor of the Aurora kinases, suppresses tumor growth *in vivo*. Nat Med 2004;10:262–7.
32. Anderson K, Yang J, Koretke K, et al. Binding of TPX2 to Aurora A alters substrate and inhibitor interactions. Biochemistry 2007;46:10287–95.
33. Gerlich D, Hirota T, Koch B, Peters JM, Ellenberg J. Condensin I stabilizes chromosomes mechanically through a dynamic interaction in live cells. Curr Biol 2006;16:333–44.
34. Lam WW, Peterson EA, Yeung M, Lavoie BD. Condensin is required for chromosome arm cohesion during mitosis. Genes Dev 2006;20:2973–84.
35. Scuric Z, Stain SC, Anderson WF, Hwang JJ. New member of aldose reductase family proteins overexpressed in human hepatocellular carcinoma. Hepatology 1998;27:943–50.
36. Teramoto R, Minagawa H, Honda M, et al. Protein expression profile characteristic to hepatocellular carcinoma revealed by 2D-DIGE with supervised learning. Biochim Biophys Acta 2008;1784:764–72.
37. Li CP, Goto A, Watanabe A, et al. AKR1B10 in usual interstitial pneumonia: expression in squamous metaplasia in association with smoking and lung cancer. Pathol Res Pract 2008;204:295–304.

Supplementary Table S1. Clinicopathological characteristics of HCC patients

	Discovery Set 1	Discovery Set 2	Validation Set 1	Validation Set 2
Total no. of patients	10	10	20	44
Age, years				
Mean (SD)	66.1 (5.9)	68 (8.9)	61.3 (10.9)	64.8 (9.9)
Sex, no. of patients (%)				
Male	10	9	16 (80)	35 (79.5)
Female	0	1	4 (20)	9 (20.5)
Hepatitis virus infection, no. of patients (%)				
No	1	1	2 (10)	9 (20.5)
B	2	5	7 (35)	12 (27.3)
C	6	3	11 (55)	20 (45.5)
B+C	1	1	0	3 (6.8)
Background liver, no. of patients (%)				
Normal	0	0	1 (5)	5 (11.4)
Chronic hepatitis (CH)	7	3	8 (40)	23 (52.3)
Liver cirrhosis (LC)	2	4	8 (40)	8 (18.2)
CH + LC	0	0	1 (5)	0
Precirrhosis	1	3	2 (10)	8 (18.2)
Tumor size, cm3				
mean (SD)	68.3 (42.0)	120.9 (218.1)	87.8 (111.9)	176.4 (256.7)
Histology, no. of patients (%)				
Well	1	0	1 (5)	5 (11.4)
Well to moderately	0	0	4 (20)	0
Moderately	5	10	8 (40)	27 (61.4)
Moderately to poorly	1	0	1 (5)	0
Poorly	3	0	6 (30)	12 (27.3)
Intrahepatic metastases, no. of patients (%)				
0	7	7	17 (85)	30 (68.2)
1	1	1	2 (10)	14 (31.8)
2	2	2	0	0
3	0	0	1 (5)	0
Portal vein involvement, no. of patients (%)				
0	4	1	10 (50)	17 (38.6)
1	5	8	7 (35)	24 (54.5)
2	0	1	0	1 (2.3)
3	1	0	3 (15)	2 (4.5)

Supplementary Table S2. List of genes up-regulated in HCC (Discovery Set 1)

Transcript Cluster ID	RefSeq	Gene symbol	*P*-value	Fold change	Gene description
2337716	NM_006252	PRKAA2	6.71E-04	4.42	Protein kinase, AMP-activated, alpha 2 catalytic subunit
2379863	NM_016343	CENPF|TUBD1|PAK1	1.05E-04	3.22	Centromere protein F, 350/400ka (mitosin) | tubulin, delta 1 | p21/Cdc42/Rac1-activated kinase 1 (STE20 homolog, yeast)
2427007	NM_002959	SORT1|PSRC1|MYBPHL	1.24E-04	3.14	Sortilin 1 | proline/serine-rich coiled-coil 1 | myosin binding protein H-like
2441386	NM_003617	RGS5|UPK1B	5.06E-06	3.27	Regulator of G-protein signalling 5 | uroplakin 1B
2449559	NM_018136	ASPM	4.37E-05	3.03	Asp (abnormal spindle) homolog, microcephaly associated (Drosophila)
2469252	NM_001034	RRM2	6.68E-06	3.36	Ribonucleotide reductase M2 polypeptide
2544201	NM_004881|NM_147184	TP53I3|PFN4	7.69E-06	3.67	Tumor protein p53 inducible protein 3 | profilin family, member 4
2784113	NM_001237	CCNA2	4.01E-04	3.43	Cyclin A2
2813414	NM_031966	CCNB1	5.02E-06	3.53	Cyclin B1
2899102	NM_003531	HIST1H3C	5.21E-05	4.94	Histone cluster 1, H3c
2946215	NM_003537	HIST1H3B	3.73E-06	4.99	Histone cluster 1, H3b
2947077	NM_003533	HIST1H3I	2.49E-05	3.61	Histone cluster 1, H3i
2997376	NM_018685	ANLN	1.43E-05	3.39	Anillin, actin binding protein
3025433	NM_020299	AKR1B10|LOC340888|LOC441282	4.50E-04	18.03	Aldo-keto reductase family 1, member B10 (aldose reductase) | similar to aldo-keto reductase family 1, member B10
3260586	NM_005063	SCD|LOC645313|LOC651109	8.76E-05	3.43	Stearoyl-CoA desaturase (delta-9-desaturase) | similar to Acyl-CoA desaturase (Stearoyl-CoA desaturase) (Fatty acid desaturase) (Delta(9)-desaturase)
3329343	NM_002391|NM_001012334|NM_001012333	MDK	4.38E-04	3.90	Midkine (neurite growth-promoting factor 2)
3375545	NM_013402	FADS1|FADS3	2.74E-04	3.34	Fatty acid desaturase 1 | fatty acid desaturase 3
3590388	NM_018454|NM_016359	NUSAP1	1.62E-05	3.09	Nucleolar and spindle associated protein 1
3756193	NM_001067	TOP2A	7.29E-06	4.63	Topoisomerase (DNA) II alpha 170kDa
3881443	NM_012112	TPX2|TINAGL1	2.10E-06	3.11	TPX2, microtubule-associated, homolog (Xenopus laevis) | tubulointerstitial nephritis antigen-like 1
3639031	NM_199414|NM_199413|NM_003981	PRC1	8.32E-06	3.17	Protein regulator of cytokinesis 1

Supplementary Table S3. List of genes down-regulated in HCC (Discovery Set 1)

Transcript Cluster ID	RefSeq	Gene symbol	*P*-value	Fold change	Gene description
2331679	NM_032793	MFSD2|LOC731362	1.37E-05	3.98	Major facilitator superfamily domain containing 2 | similar to ribosomal protein S2
2337786	NM_000562	C8A	6.13E-04	3.77	Complement component 8, alpha polypeptide
2377332	NM_000651|NM_000573	CR1|LOC653907	3.69E-08	3.32	Complement component (3b/4b) receptor 1 (Knops blood group) | similar to complement component (3b/4b) receptor 1 isoform F precursor
2388085	NM_003679	KMO	2.13E-04	3.96	Kynurenine 3-monooxygenase (kynurenine 3-hydroxylase)
2403080	NM_003665|NM_173452	MAP3K6|FCN3	4.00E-09	18.47	Mitogen-activated protein kinase kinase kinase 6 | ficolin (collagen/fibrinogen domain containing) 3 (Hakata antigen)
2439138	NM_005894	CD5L	1.52E-06	12.18	CD5 molecule-like
2443120	NM_001937	DPT	4.15E-07	5.63	Dermatopontin
2475911	NM_014600	EHD3	3.24E-09	3.30	EH-domain containing 3
2502686	NM_006770	MARCO	8.19E-10	6.79	Macrophage receptor with collagenous structure
2547231	NM_000348	SRD5A2	7.70E-05	4.20	Steroid-5-alpha-reductase, alpha polypeptide 2 (3-oxo-5 alpha-steroid delta 4-dehydrogenase alpha 2)
2678298	NM_004944	DNASE1L3|ACTB	5.72E-07	9.65	Deoxyribonuclease I-like 3 | actin, beta
2693620	NM_144639	UROC1	2.30E-06	6.38	Urocanase domain containing 1
2716124	NM_001528	HGFAC	9.54E-07	4.84	HGF activator
2729852	NM_005953	MT2A|MT1M|LOC441019|NUTF2	1.53E-04	3.38	Metallothionein 2A | metallothionein 1M | hypothetical gene supported by X97260; BC070289 | nuclear transport factor 2
2745899	NM_022475	HHIP	7.34E-08	3.97	Hedgehog interacting protein
2772566	NM_144646	IGJ	4.02E-04	7.76	Immunoglobulin J polypeptide, linker protein for immunoglobulin alpha and mu polypeptides
2773434	NM_002089	CXCL2	1.94E-05	5.90	Chemokine (C-X-C motif) ligand 2
2775259	NM_152545	RASGEF1B|ALK|RBM41	6.25E-05	3.25	RasGEF domain family, member 1B | anaplastic lymphoma kinase (Ki-1) | RNA binding motif protein 41
2775390		MOP-1	8.90E-04	3.53	
2775909	NM_016619	PLAC8	7.54E-11	13.74	Placenta-specific 8
2792127	NM_000909	NPY1R|LOC729743|LOC731120	6.08E-09	3.06	Neuropeptide Y receptor Y1 | similar to neuropeptide Y receptor Y1
2794584	NM_005277|NM_201591|NM_201592	GPM6A|MPDU1	9.68E-09	3.47	Glycoprotein M6A | mannose-P-dolichol utilization defect 1
2807716	NM_000587	C7	2.60E-05	11.43	Complement component 7
2816536	NM_001882	CRHBP	3.45E-09	13.85	Corticotropin releasing hormone binding protein
2842624	NM_017675	PCLKC	6.73E-04	4.88	Protocadherin LKC
2853055	NM_031900	AGXT2	4.55E-04	3.61	Alanine-glyoxylate aminotransferase 2
2854092	NM_002310	LIFR	2.95E-07	7.18	Leukemia inhibitory factor receptor alpha
2854409	NM_001737	C9|ASTN2	7.35E-05	16.46	Complement component 9 | astrotactin 2
2876608	NM_004887	CXCL14	8.13E-08	4.89	Chemokine (C-X-C motif) ligand 14
2883283	NM_138379	TIMD4	3.38E-08	4.36	T-cell immunoglobulin and mucin domain containing 4
2907513	NM_018960	GNMT	1.61E-04	6.98	Glycine N-methyltransferase
2955761	NM_016593	CYP39A1	6.59E-04	3.97	Cytochrome P450, family 39, subfamily A, polypeptide 1
2975257	NM_022568|NM_170771	ALDH8A1|HBS1L	7.13E-04	3.41	Aldehyde dehydrogenase 8 family, member A1 | HBS1-like (S. cerevisiae)
2982630	NM_024492|NM_145727	LPAL2|LOC732058|PLGLB2	5.06E-05	3.86	Lipoprotein, Lp(a)-like 2 | similar to Apolipoprotein(a) precursor (Apo(a)) (Lp(a)) | plasminogen-like B2
2982730	NM_005577	LPA|LOC732390|LOC732436|PLGLB2|TMEM166	8.05E-06	7.98	Llipoprotein, Lp(a) | similar to Apolipoprotein(a) precursor (Apo(a)) (Lp(a)) | plasminogen-like B2 | transmembrane protein 166

2995476		INMT	1.51E-05	3.47	Indolethylamine N-methyltransferase
3049292	NM_001013398|NM_000598	IGFBP3	4.56E-05	4.96	Insulin-like growth factor binding protein 3
3058944	NM_001010932|NM_000601|NM_001010931|NM_001010933|NM_001010934	HGF	1.38E-05	5.69	Hepatocyte growth factor (hepapoietin A; scatter factor)
3060332	NM_024636	STEAP4	5.41E-06	3.70	STEAP family member 4
3065740	NM_173054|NM_005045	RELN	3.74E-04	5.62	Reelin
3095257	NM_194294	INDOL1	2.39E-04	3.08	Indoleamine-pyrrole 2,3 dioxygenase-like 1
3095313	NM_020130	C8orf4	1.82E-07	3.76	Chromosome 8 open reading frame 4
3113133	NM_006438	COLEC10	1.37E-06	13.60	Collectin sub-family member 10 (C-type lectin)
3128817	NM_000680|NM_033303|NM_033304|NM_033302	ADRA1A	1.87E-04	3.71	Adrenergic, alpha-1A-, receptor
3193631	NM_004108|NM_015837	FCN2	1.70E-07	3.64	Ficolin (collagen/fibrinogen domain containing lectin) 2 (hucolin)
3204285	NM_006274	CCL19	4.46E-05	11.65	Chemokine (C-C motif) ligand 19
3204301	NM_002989	CCL21	1.51E-04	4.04	Chemokine (C-C motif) ligand 21
3215570	NM_000507	FBP1	2.86E-04	3.65	Fructose-1,6-bisphosphatase 1
3237286	NM_001009567	MRC1	1.08E-06	4.72	Mannose receptor, C type 1
3251566	NM_152635	OIT3|C1orf146	2.82E-08	10.95	Oncoprotein induced transcript 3 | chromosome 1 open reading frame 146
3286602	NM_000609|NM_199168|NM_001033886	CXCL12	3.57E-06	5.02	Chemokine (C-X-C motif) ligand 12 (stromal cell-derived factor 1)
3302533	NM_003015	SFRP5	1.38E-05	4.31	Secreted frizzled-related protein 5
3333811	NM_001039752	SLC22A10	3.50E-04	5.11	Solute carrier family 22 (organic anion/cation transporter), member 10
3348940	NM_031938|NM_001037290	KCTD9|BCDO2|LOC728291|LOC642513|LOC728707|LOC729404|LOC730942|LOC650978|LOC647852|LOC731540	3.85E-05	4.40	Potassium channel tetramerisation domain containing 9 | beta-carotene dioxygenase 2 | similar to potassium channel tetramerisation domain containing 9 | hypothetical protein LOC728707
3349858	NM_006169	NNMT	2.28E-05	9.79	Nicotinamide N-methyltransferase
3359121	NR_003512|NM_001007139|NM_000612	INS-IGF2	7.64E-04	13.10	Insulin- insulin-like growth factor 2 | insulin-like growth factor 2 (somatomedin A)
3360401	NM_000518	HBB	3.13E-06	3.35	Hemoglobin, beta
3362826	NM_006691	XLKD1	6.72E-09	8.65	Extracellular link domain containing 1
3365318	NM_006512	SAA4	9.90E-04	3.56	Serum amyloid A4, constitutive
3374934	NM_152852|NM_022349|NM_152851	MS4A6A|LOC643680	2.47E-05	3.25	Membrane-spanning 4-domains, subfamily A, member 6A | hypothetical protein
3402786	NM_000616	CD4|S100PBP	1.43E-06	3.07	CD4 molecule | S100P binding protein
3426257	NM_003877	SOCS2	6.46E-04	4.70	Suppressor of cytokine signaling 2
3428573	NM_152323	SPIC|LOC646120	2.74E-05	3.06	Spi-C transcription factor (Spi-1/PU.1 related) | similar to Spi-C transcription factor (Spi-1/PU.1 related)
3429159	NM_017564	STAB2	3.97E-09	9.37	Stabilin 2
3442706	NM_004244|NM_203416	CD163	9.19E-06	4.07	
3443936	NM_016509	CLEC1B	1.47E-10	6.14	C-type lectin domain family 1, member B
3457794	NM_001638	APOF|STAT2	7.09E-04	10.21	Apolipoprotein F | signal transducer and activator of transcription 2, 113kDa
3457891	NM_013267	GLS2	9.06E-06	8.54	Glutaminase 2 (liver, mitochondrial)
3465274	NM_001920|NM_133503|NM_133504|NM_133505|NM_133506|NM_133507	DCN	2.73E-05	8.72	Decorin

3466687	NM_002108	HAL	8.59E-04	4.82	Histidine ammonia-lyase
3468345	NM_000618	IGF1	9.19E-04	5.16	Insulin-like growth factor 1 (somatomedin C)
3472366	NM_006843	SDS	7.40E-05	11.63	Serine dehydratase
3486096	NM_207361	FREM2	3.91E-04	4.61	FRAS1 related extracellular matrix protein 2
3502475	NM_003891	PROZ	7.77E-05	3.30	Protein Z, vitamin K-dependent plasma glycoprotein
3544525	NM_005252	FOS	5.63E-04	5.88	V-fos FBJ murine osteosarcoma viral oncogene homolog
3565524	NM_000161|NM_001024024|NM_001024070|NM_001024071	GCH1|LOC202181	2.98E-06	3.49	GTP cyclohydrolase 1 (dopa-responsive dystonia) | hypothetical protein LOC202181
3642664	NM_000517	HBA2|HBA1	2.14E-05	3.01	Hemoglobin, alpha 2 | hemoglobin, alpha 1
3651478	NM_005622|NM_202000	ACSM3	2.19E-04	4.11	Acyl-CoA synthetase medium-chain family member 3
3661940	NM_020988|NM_138736	GNAO1	2.93E-05	5.01	Guanine nucleotide binding protein (G protein), alpha activating activity polypeptide O
3662139	NM_175617	MT1E|MT1M|MT1A|NUTF2	6.83E-04	7.58	Metallothionein 1E (functional) | metallothionein 1M | metallothionein 1A (functional) | nuclear transport factor 2
3662150	NM_176870	MT1M|MT1JP|NUTF2	6.55E-04	6.69	Metallothionein 1M | metallothionein 1J (pseudogene) | nuclear transport factor 2
3662158		C20orf127|MT1JP|NUTF2	5.85E-04	5.65	Chromosome 20 open reading frame 127 | metallothionein 1J (pseudogene) | nuclear transport factor 2
3662201	NM_005951|NM_005949|NM_001039954	MT1F|MT1H|LOC645745|LOC727730|MT1A|NUTF2	6.89E-04	6.17	Metallothionein 1F (functional) | metallothionein 1H | metallothionein 1H-like protein | similar to metallothionein 1H-like protein | metallothionein 1A (functional) | nuclear transport factor 2
3662247	NM_005952	MT1X|MT1A|NUTF2	3.34E-04	4.93	Metallothionein 1X | metallothionein 1A (functional) | nuclear transport factor 2
3662417	NM_000078	CETP	1.44E-07	6.67	Cholesteryl ester transfer protein, plasma
3667811	NM_001361	DHODH	5.29E-05	3.68	Dihydroorotate dehydrogenase
3692999	NM_005950	MT1G|NUTF2	8.51E-04	8.16	Metallothionein 1G | nuclear transport factor 2
3696035	NM_000229	LCAT	1.50E-05	3.98	Lecithin-cholesterol acyltransferase
3742627		UNQ5783	2.48E-07	3.26	DTFT5783
3748798	NM_002404	MFAP4	1.01E-05	4.91	Microfibrillar-associated protein 4
3768627	NM_007168	ABCA8	8.15E-04	3.23	ATP-binding cassette, sub-family A (ABC1), member 8
3793827	NM_032649	CNDP1	2.87E-05	4.19	Carnosine dipeptidase 1 (metallopeptidase M20 family)
3819130	NM_214677|NM_214678|NM_214679|NM_014257|NM_214676|NM_214675	CLEC4M	8.20E-09	13.16	C-type lectin domain family 4, member M
3830306	NM_021175	HAMP	8.23E-09	52.87	Hepcidin antimicrobial peptide
3848525	NM_198492	CLEC4G	6.15E-10	6.21	C-type lectin superfamily 4, member G
3881391	NM_181353|NM_002165	ID1	3.28E-06	6.01	Inhibitor of DNA binding 1, dominant negative helix-loop-helix protein
3883233		C20orf127|MT1JP|MT1M|MT1A	6.22E-04	5.41	Chromosome 20 open reading frame 127 | metallothionein 1J (pseudogene) | metallothionein 1M | metallothionein 1A (functional)
3890640	NM_002591	PCK1	9.83E-04	7.09	Phosphoenolpyruvate carboxykinase 1 (soluble)
3974019	NM_004615	TSPAN7	6.45E-04	3.16	Tetraspanin 7
4007164	NM_002621	CFP	5.21E-10	3.72	Complement factor properdin
4011008	NM_007268	EIF4B|VSIG4|LOC643873|LOC339881|LOC645430|LOC392485|LOC650271|THRSP	5.70E-05	3.50	Eukaryotic translation initiation factor 4B | V-set and immunoglobulin domain containing 4 | similar to eukaryotic translation initiation factor 4B | hypothetical LOC645430 | similar to ataxin 7-like 3 | hypothetical protein LOC650271 | thyroid hormone responsive (SPOT14 homolog, rat)
4020655	NM_014253	ODZ1	8.93E-04	3.60	Odz, odd Oz/ten-m homolog 1(Drosophila)
4027639	NM_000132|NM_019863	F8	1.69E-05	3.01	Coagulation factor VIII, procoagulant component (hemophilia A)

Supplementary Table S4. List of siRNA

Gene symbol	ID
AKR1B10	43766
	133050
	112090
ANLN	132619
	132620
	132621
CCNB1	118838
	118839
DEPDC1	148669
	148670
	148671
HCAP-G	125362
	125363
	125364
HIST1H3B	214117
	214118
	214119
HIST1H3C	13270
	45052
	44958
HIST1H3I	13272
	44960
	45054
RRM2	9302
	110819
	110822
TPX2	19774
	136425
	136426

Supplementary Table S5. List of TaqMan Gene Expression Assays

Gene symbol	Assay ID
AKR1B10	Hs00252524_m1
ANLN	Hs00218803_m1
C7	Hs00175109_m1
CCNA2	Hs00153138_m1
COLEC10	Hs00197571_m1
CRHBP	Hs00181810_m1
HAMP	Hs00221783_m1
HCAP-G	Hs00254617_m1
HIST1H3I	Hs00605800_s1
RGS5	Hs00186212_m1
RRM2	Hs00357247_g1
TPX2	Hs00201616_m1

Supplementary Table S6. Effects of siRNA treatment on the growth of xenografts

	Estimate*	Standard error*	*t*-Value	Adjusted *P*-value
Control (Intercept)	3.744	0.189		
TPX2	-1.239	0.161	-7.699	< 0.001
RRM2	-1.153	0.168	-6.878	< 0.001
AKR	-0.499	0.162	-3.088	0.012
HCAPG	-0.782	0.168	-4.667	< 0.001

*On a natural logarithmic scale.

Research Article

Molecular Cancer Therapeutics

Reduced Argininosuccinate Synthetase Is a Predictive Biomarker for the Development of Pulmonary Metastasis in Patients with Osteosarcoma

Eisuke Kobayashi[1,4], Mari Masuda[1], Robert Nakayama[2,4], Hitoshi Ichikawa[2], Reiko Satow[1], Miki Shitashige[1], Kazufumi Honda[1], Umio Yamaguchi[1,5], Ayako Shoji[6], Naobumi Tochigi[3], Hideo Morioka[4], Yoshiaki Toyama[4], Setsuo Hirohashi[1], Akira Kawai[5], and Tesshi Yamada[1]

Abstract

Pulmonary metastasis is the most significant prognostic determinant for osteosarcoma, but methods for its prediction and treatment have not been established. Using oligonucleotide microarrays, we compared the global gene expression of biopsy samples between seven osteosarcoma patients who developed pulmonary metastasis within 4 years after neoadjuvant chemotherapy and curative resection, and 12 patients who did not relapse. We identified argininosuccinate synthetase (*ASS*) as a gene differentially expressed with the highest statistical significance (Welch's t test, $P = 2.2 \times 10^{-5}$). Immunohistochemical analysis of an independent cohort of 62 osteosarcoma cases confirmed that reduced expression of ASS protein was significantly correlated with the development of pulmonary metastasis after surgery (log-rank test, $P < 0.05$). Cox regression analysis revealed that ASS was the sole significant predictive factor ($P = 0.039$; hazard ratio, 0.319; 95% confidence interval, 0.108-0.945). ASS is one of the enzymes required for the production of a nonessential amino acid, arginine. We showed that osteosarcoma cells lacking ASS expression were auxotrophic for arginine and underwent G_0-G_1 arrest in arginine-free medium, suggesting that an arginine deprivation therapy could be effective in patients with osteosarcoma. Recently, phase I and II clinical trials in patients with melanoma and hepatocellular carcinoma have shown the safety and efficacy of plasma arginine depletion by stabilized arginine deiminase. Our data indicate that in patients with osteosarcoma, reduced expression of ASS is not only a novel predictive biomarker for the development of metastasis, but also a potential target for pharmacologic intervention. *Mol Cancer Ther; 9(3); 535–44. ©2010 AACR.*

Introduction

Although rare (200–300 newly diagnosed cases per year in Japan), osteosarcoma is the most frequent primary malignant bone tumor, developing mainly in the metaphysis of long bones of children and young adults. The introduction of preoperative high-dose combined chemotherapy in the last three decades has significantly improved the disease-free 5-year survival rate of young (ages <40 years) patients with osteosarcoma of the extremities to approximately 50% to 80% (1). However, a significant proportion of osteosarcoma patients develop metastasis even after curative resection of the primary tumor (1, 2). The lung is the most common organ to which osteosarcoma metastasizes first. Solitary metastasis can be treated by lung resection, but suitable management of patients with multiple pulmonary metastases has not been established. Furthermore, metastatic osteosarcoma often develops resistance to chemotherapeutic agents that were initially effective for treatment of the primary tumor. Osteosarcoma patients with lung metastasis have a poor prognosis, with an overall survival rate of <30% (3). Development of lung metastasis is the most significant determinant of poor prognosis in osteosarcoma, followed by poor response to neoadjuvant chemotherapy (1). Because such high-risk patients may derive some benefit from modification (intensification) of their preoperative and postoperative therapeutics, the development of a reliable diagnostic method that can stratify osteosarcoma patients according to their likelihood of developing lung metastasis would be highly valuable.

Various prognostic clinicopathologic factors have been reported, including patient age, tumor size, histologic subtype, and site of origin (1). The proximal and axial location of osteosarcoma significantly affects the outcome

Authors' Affiliations: [1]Chemotherapy, [2]Genetics, and [3]Pathology Divisions, National Cancer Center Research Institute; [4]Department of Orthopaedic Surgery, Keio University; [5]Orthopaedic Division, National Cancer Center Hospital; and [6]BioBusiness Group, Mitsui Knowledge Industry, Tokyo, Japan

Note: Supplementary material for this article is available at Molecular Cancer Therapeutics Online (http://mct.aacrjournals.org/).

Microarray analysis: Microarray data of this study have been submitted to the Gene Expression Omnibus database (accession number GSE14827).

Corresponding Author: Mari Masuda, Chemotherapy Division, National Cancer Centre Research Institute, 5-1-1 Tsukiji, Chuo-ku, Tokyo 104-0045, Japan; Phone: 81-3-3542-2511; Fax: 81-3-3547-6045. E-mail: mamasuda@ncc.go.jp

doi: 10.1158/1535-7163.MCT-09-0774

©2010 American Association for Cancer Research.